Green Chemistry

PAPER

View Article Online
View Journal



Cite this: DOI: 10.1039/d6gc00369a

# Upcycling silicon from End-of-Life photovoltaic panels to a heterogeneous catalyst for the Mizoroki–Heck cross-coupling

Giulia Brufani,[a] Marco Mearelli,[b] Filippo Campana,[b] Nicola Taurisano,[c] Maria Lucia Protopapa[c] and Luigi Vaccaro *[b]

Received 19th January 2026,
Accepted 2nd April 2026

DOI: 10.1039/d6gc00369a

rsc.li/greenchem

Beyond the global shift toward solar-derived renewable energy sources, a significant concern has also emerged. With an average lifetime of 25–30 years, global photovoltaic (PV) waste is expected to account for 8 million tons of total installed by 2030. Consequently, the challenge of managing the enormous volume of End-of-Life (EoL) PV modules is emerging as a significant environmental issue for the coming decades. High-purity, energy-intensive silicon wafers account for about 3–4% of a photovoltaic module's total weight and represent a significant fraction of its total cost. Consequently, the development of effective strategies to upcycle silicon scraps from discarded solar panels is urgently needed. Herein, we propose a circularly driven waste-to-wealth strategy for a novel application for the globally growing EoL solar panel waste streams, using Si as a heterogeneous support for Pd nanoparticle-based catalytic systems. We have achieved excellent performance in the Mizoroki–Heck reaction, comparable to, or even better than, that of well-established Pd-based heterogeneous catalysts, in terms of catalytic activity, minimal palladium leaching, and excellent recyclability. 20 different products have been prepared, including an intermediate for the synthesis of an Lp-PLA$_2$ inhibitor, methyl (*E*)-ferulate, and a rilpivirine intermediate.

**Green foundation**

1. This study presents a strategy for managing the rapidly increasing global EoL solar panel waste stream by purposing recovered silicon as a heterogeneous support for a Pd-nanoparticle catalytic system, achieving performances comparable to established Pd-based heterogeneous catalysts.
2. Recycling costly solar-grade silicon provides a quantifiable advantage for the sustainable management of EoL photovoltaic waste. The newly developed Pd/Si catalyst was successfully reused for 6 consecutive Mizoroki–Heck runs, showing Pd-leaching levels comparable to those of the benchmark Pd/C catalyst, as well as similar TON and TOF values. The *E*-factor was further assessed to 8.5.
3. This work paves the way for the broader use of silicon derived from EoL photovoltaic as a versatile heterogeneous support for a wide range of metal-based catalytic systems, thereby expanding the possibilities for their application across diverse catalytic processes.

## Introduction

Solar energy drives the global transition toward renewable energy sources, marking a shift away from fossil fuels and accounting for 81% of all renewable capacity added worldwide.[1–3] Photovoltaic (PV) technology has experienced significant growth over the past few decades. The year 2024 marked a milestone year for solar power, with global photovoltaic installations surging by 33% to reach a record of 597 GW.[4] Projections anticipate substantial global growth in solar PV production, reaching over 1630 GW by 2030 and a remarkable 4500 GW by 2050.[5]

However, there is a concerning downside. With an average lifetime of 25–30 years, global PV waste is expected to account for 4–14% of total installed capacity by 2030, reaching a global waste volume estimated at around 8 million tons by 2030 and surging to over 80% (an estimated 60–78 million tonnes) by 2050.[6–8] Consequently, the challenge of managing the enormous volume of End-of-Life (EoL) PV modules is beginning to emerge as a significant environmental issue for the coming decades.[9]

To address environmental issues arising from the increasing volume of discarded electronic devices, the European

[a]*Department of Civil, Energy, Environmental and Material Engineering (DICEAM), Università degli Studi Mediterranea di Reggio Calabria, Via Graziella, Feo di Vito, Reggio Calabria 89122, Italy*
[b]*Laboratory of Green S.O.C. – Dipartimento di Chimica, Biologia e Biotecnologie, Università degli Studi di Perugia, Via Elce di Sotto 8, Perugia 06123, Italy. E-mail: luigi.vaccaro@unipg.it*
[c]*Italian National Agency for New Technologies, Energy and Sustainable Economic Development (ENEA), Laboratory Technologies for Waste and Secondary Raw Materials (RMP), Division Circular Economy (EC), Department for Sustainability (SSPT), Brindisi Research Center, S.S. 7 Appia km 706, 72100 Brindisi, Italy*

Union has enacted the Waste Electrical and Electronic Equipment (WEEE) Directive. This directive aims to promote a circular economy by ensuring the proper treatment of such waste.[10–13] Notably, PV panels are included within the directive's scope, mandating proper storage and recycling to prevent environmental contamination by hazardous materials and to facilitate resource recovery.[14] This inclusion underscores the importance of exploring circular economy strategies within the PV industry,[15] encouraging the design of products with recyclability as a key consideration.[16–20]

Waste generated from silicon-based EoL-PV modules comprises not only conventional materials such as glass (70%), the polymer-based EVA encapsulation layer (5.1%), the polymeric backsheet (1.5%), aluminium frames (18%), and cables containing copper and polymers (1%), but also other metals, including aluminium internal conductors (0.53%), copper (0.11%), silver and lead (0.11%), as well as high-purity, energy-intensive silicon wafers (3.65%).[18,20,21]

Life cycle assessment (LCA) studies suggest that recycling EoL PV can preserve the energy investment made during production, reduce $CO_2$ emissions throughout the entire life cycle, and mitigate resource depletion.[21–23]

Cost assessment studies indicate that silicon wafers constitute a major contribution to the total cost of a PV module. While metallurgical-grade silicon is priced at approximately USD $2 per kilogram, solar-grade silicon reaches around USD $9 per kilogram, and its price fluctuates and is geographically segmented.[24] The production of solar-grade silicon feedstocks thus represents one of the most significant economic and environmental burdens in the PV industry.[25,26] Implementing effective recycling strategies for end-of-life PV modules can substantially improve the industry's overall sustainability.[27]

Several industrial processes exist aiming to separate key components, including glass, ethyl vinyl acetate (EVA), silicon, and the backsheet.[28] Mechanical methods (*e.g.*, shredding) are fast and suitable for large-scale applications, but they often produce mixed and contaminated output streams. Thermal processes, such as pyrolysis or carbonisation in air, enable cleaner separation but require a high energy input and strict control of gas emissions.[29] Chemical delamination, which utilises solvents to dissolve the EVA encapsulant, facilitates the recovery of high-purity materials at lower temperatures; however, it presents challenges related to solvent costs, toxicity, and recovery. The selection of the most appropriate recycling technology should be based on identifying the hazardous substances and recyclable materials contained in the PV module structure.[30,31] Regardless of the method used, recovered silicon typically remains contaminated with metals and requires additional purification steps to reach the target purity, depending on the intended reuse application.[32]

Silicon recovered from disposed PV modules is rarely reused in the solar industry, primarily due to wafer breakage and contamination (*e.g.*, dopants, Ag/Al coatings, EVA residues). Moreover, solar-grade silicon, used in solar panels, requires ultra-high purity (≥99.9999%), and the energy and cost required to reprocess recycled Si often exceed those of using virgin material.[16,33,34]

Given these challenges, innovative technologies to upcycle Si scraps from discarded solar panels are urgently needed.[35]

In addition, it is of strategic utility to identify alternative, useful, and specific large-scale applications for exploiting the properties and structure of the very large amounts of silicon recovered from EoL PV modules that are not energetically, economically, or practically convenient to reconsider for producing efficient PV panels.

With our continued interest in the valorisation of waste to access low-cost heterogeneous Pd-catalysts for cross-coupling,[36–39] the use of silicon derived from EoL PV as a support for Pd-nanoparticles is introduced for the first time (Fig. 1).

Although silica-based heterogeneous catalysts are well established,[40–43] the application of silicon in catalysis is scarcely, if not, investigated.[44,45]

In this work, following the thermomechanical removal of the front glass, a chemical delamination process was applied to separate the silicon cells from the backsheet. Subsequently, the silicon was chemically purified to remove aluminium from the rear contact and silver from the front surface conductive fingers.

The objective of this work is to demonstrate that Si-based supports can be effectively utilised in the upcycling of Si by developing a Pd/Si catalytic system, considering that Pd/C is arguably one of the most widely used heterogeneous catalytic systems in industry.

We have decided to evaluate the utility and efficiency of this catalytic system in a widely useful benchmark Mizoroki–Heck reaction. We have decided to compare its behaviour with that of traditional catalysts, such as Pd/C, focusing on catalytic activity, palladium leaching, and recyclability.

We have also evaluated the utility of the catalyst by using it to prepare industrially relevant products, natural compounds, and intermediates for active pharmaceutical ingredients (APIs), underscoring its potential as a sustainable and promising catalyst for possible applications.

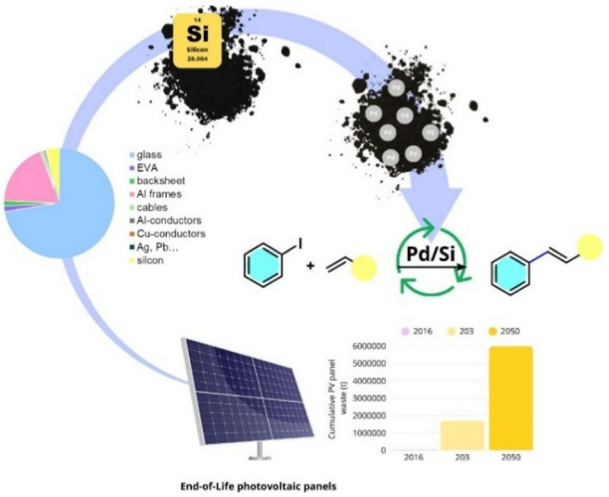


**Fig. 1** From Si, derived from End-of-Life photovoltaics, to a Pd-based heterogeneous catalyst for the Mizoroki–Heck reaction.

With our ongoing interest in replacing toxic solvents with more environmentally friendly alternatives, we decided to use biomass-derived γ-valerolactone (GVL) as a safe reaction medium, further aligning with the circular perspective.[46–49]

## Results and discussion

We initiated our study by preparing the catalyst from crystalline silicon EoL photovoltaic modules recovered from a discarded solar panel. The process began with delamination to extract the silicon from the solar cell, followed by leaching treatments to remove residual Al and Ag, and subsequent milling to obtain a fine Si powder (Si_EoLPV) with an 86 wt% purity (see SI for further information). Next, the Si powder is dispersed in diethylene glycol, and an *in situ*-generated $H_2PdCl_4$ precursor is introduced. The suspension's pH was adjusted to 10–12, and the reduction of Pd was carried out at 130 °C under an argon atmosphere, leading to the immobilisation of Pd nanoparticles on the Si support. The same procedure was followed for catalyst preparation, using commercial metallurgical-grade Si powder (99 wt% purity) purchased from Merck.

The performance of the recovered-Si-based catalyst, Pd/Si_EoLPV, is compared with that of an analogous catalyst prepared using commercial metallurgical-grade Si powder, Pd/Si. MP-AES analysis revealed a Pd content of 2.7 wt% for Pd/Si and 3.0 wt% for Pd/Si_EoLPV.

The Pd/Si and Pd/Si_EoLPV catalysts were characterised by STEM and EDS, revealing the formation of Pd nanoparticles (NPs) with average particle sizes of 3.6 ± 1.1 and 3.8 ± 1.2 nm, respectively (Fig. 2i and ii). XPS analysis shows intense Pd 3d signals, mainly composed of Pd in the oxidation states Pd(0) at a binding energy of 335.6 eV and Pd(II) at 337.8 eV, with a $Pd^0/Pd^{2+}$ ratio of approximately 5. The Pd $3d_{5/2}$ and Pd $3d_{3/2}$ components exhibit a doublet spin–orbit coupling (DSOC) of 5.2 eV for both Pd(0) and Pd(II), as expected for these catalysts (Fig. 2iii). Analysis of the Si 2p region reveals only the contribution associated with oxidised silicon ($Si^{4+}$) for both catalysts (Fig. 2iii and iv). The Pd nanoparticles obtained on both silicon supports, each used as a precursor for catalyst preparation *via* the polyol method, are highly similar, with no significant differences in particle size, morphology, or dispersion.

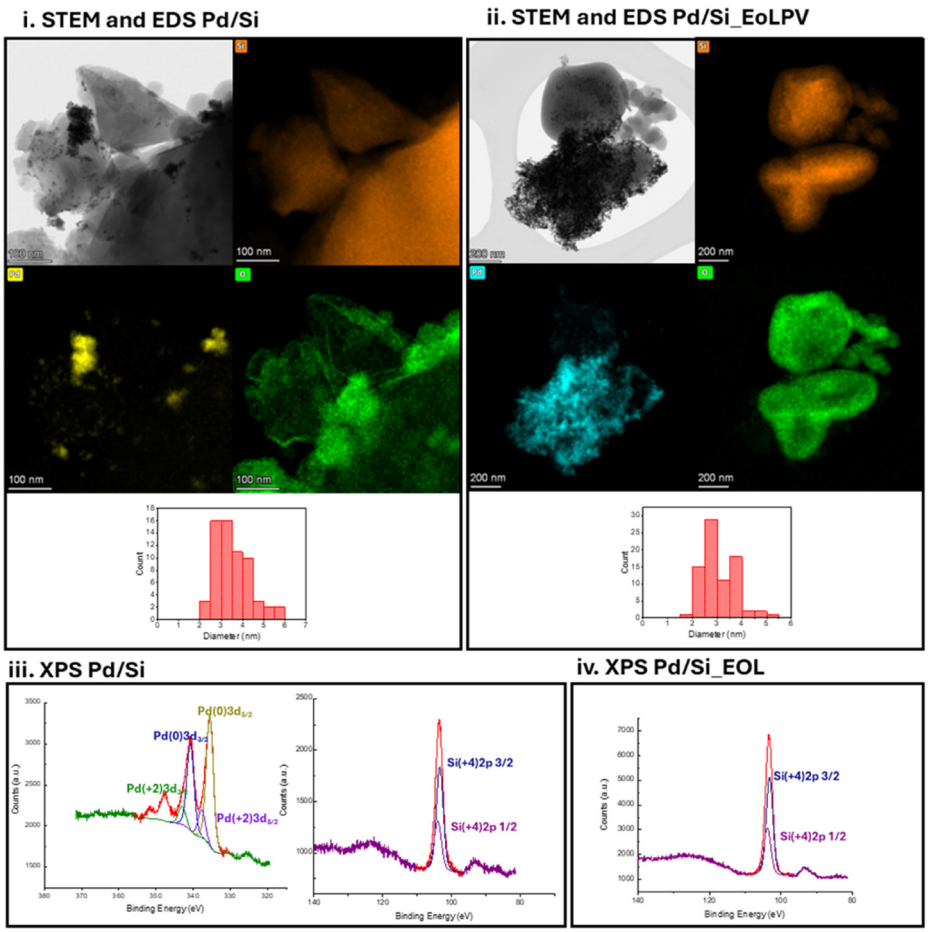


**Fig. 2** (i) STEM and EDS images and the nanoparticle size distribution of Pd/Si. (ii) STEM and EDS images and the nanoparticle size distribution of Pd/Si_EoLPV. (iii) XPS spectrum of Pd 3d region for Pd/Si and Si 2p region for Pd/Si. (iv) XPS spectrum of Pd 3d region for Pd/Si and Si 2p region for Pd/Si.

This indicates that the origin of the silicon support does not appreciably influence the formation or structural characteristics of the Pd nanoparticles under the applied conditions.

The catalytic efficiency of the Pd/Si catalyst was evaluated in the Mizoroki–Heck reaction of iodobenzene (**1a**) and methyl acrylate (**2a**) using triethylamine (TEA) as an organic base. We began the optimisation by screening the waste-derived solvent cyclopentyl methyl ether (CPME), which resulted in unsatisfactory conversion (Table 1, entry 1).[50–54] We then tested bio-based solvents, including 2-methyltetrahydrofuran (2-MeTHF) (Table 1, entry 2),[55,56] furfuryl alcohol (FA) (Table 1, entry 3),[57] and GVL (Table 1, entry 4). Among these, GVL demonstrated superior efficiency, achieving complete conversion. The conventional reaction mediums dimethyl formamide (DMF) and dimethyl acetamide (DMA) did not provide complete conversion (Table 1, entries 5 and 6).

Inorganic bases $Na_2CO_3$ and $K_2CO_3$ did not provide complete conversion due to their lower solubility in GVL (Table 1, entries 7 and 8), whereas $Cs_2CO_3$ afforded complete conversion (Table 1, entry 9). Heterogeneous bases, PS-TEA, PS-MEA, and PS-piperidinomethyl, afforded complete conversion (Table 1, entries 10–12). In line with a sustainability-driven approach, iodobenzene (**1a**) was selected over bromobenzene and chlorobenzene to ensure efficient reactivity under mild conditions. Its superior reactivity enables the use of a simple, ligand-free heterogeneous catalyst, thereby avoiding costly and waste-generating ligand systems. This strategy reduces both environmental impact and process complexity, aligning with more sustainable and industrially relevant cross-coupling practices.[58] Notably, when the optimised conditions were applied using chlorobenzene or bromobenzene in place of iodobenzene (**1a**), no conversion was observed.

A blank experiment performed using Si_EoLPV, in the absence of Pd, did not promote the coupling reaction, confirming that residue metal does not contribute to the coupling reaction (Table 2, entry 1). The reaction performed with homogeneous TEA determined a Pd leaching of 2.6 ppm (Table 2, entry 2). This value decreased to 1.6 ppm when a heterogeneous base was used (Table 2, entry 3). Lowering the reaction temperature to 120 °C resulted in an increased Pd leaching (Table 2, entry 4). Comparable results were obtained using Pd/Si_EoLPV, indicating that the catalytic activity and the leaching were unaffected by the specific source of Si used (Table 2, entries 5 and 6).

It is worthy to notice that data of Pd leaching in GVL of the novel Si-based catalyst are very encouraging and similar but even better (lower) than those observed with the commercially available Pd/C catalyst.

Specifically, under the same conditions, Pd/C led to a 8.9 ppm leaching in GVL using TEA as base while Pd/Si only 2.6–2.7 ppm (Table 2, entry 6 *vs.* entries 2 and 5).[47] Again, Pd/C leaching was 2.6 ppm when the reaction was performed with PS-TEA, while with Pd/Si a lower leaching of 1.6–1.9 ppm was achieved (Table 2, entry 8 *vs.* entries 3 and 6).

The leaching behaviour of Si-based catalysts was compared to that of $Pd/SiO_2$ prepared using the same procedure. The reaction catalysed by $Pd/SiO_2$, proceeded to complete conversion to **3a** in 16 h. Moreover, the catalyst yielded a 48 ppm leaching with TEA (Table 2, entry 9) and 9.0 ppm with PS-TEA (Table 2, entry 10). These results highlight the advantage of using silicon as a precursor for preparing Pd nanoparticle supports compared to activated mesoporous silica (60 Å, 230–400 mesh). This behavior can be attributed to the higher surface acidity of silica, arising from the presence of exposed

**Table 1** Optimisation of the reaction conditions for Pd/Si-catalysed Mizoroki–Heck cross-coupling[a]

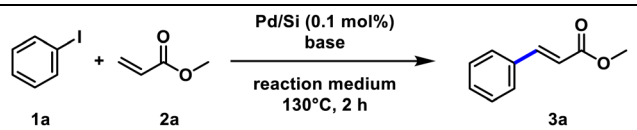


| Entry | Reaction medium | Base | $C^b$ (%) |
|---|---|---|---|
| 1 | CPME | TEA | 23 |
| 2 | 2-MeTHF | TEA | 60 |
| 3 | FA | TEA | 45 |
| 4 | GVL | TEA | >99 |
| 5 | DMF | TEA | 89 |
| 6 | DMA | TEA | 87 |
| 7 | GVL | $Na_2CO_3$ | 70 |
| 8 | GVL | $K_2CO_3$ | 40 |
| 9 | GVL | $Cs_2CO_3$ | >99 |
| 10[c] | GVL | PS-TEA | >99 |
| 11[c] | GVL | PS-MEA | >99 |
| 12[c] | GVL | PS-piperidinomethyl | >99 |

[a] Reaction condition: Pd/Si (2.7 wt%, 0.1 mol%), **1a** (1 mmol), **2a** (1.2 equiv., 1.2 mmol), base (1 equiv., 1 mmol), reaction medium (0.8 M), 130 °C, 2 h. [b] Conversion was determined by gas–liquid chromatography. The remaining material is unreacted **1a**. [c] Base (1.5 equiv., 1.5 mmol).

**Table 2** Analysis of Pd leaching (ppm) comparing Pd/Si, Pd/C, and Pd/$SiO_2$ applied with TEA and PS-TEA as bases[a]

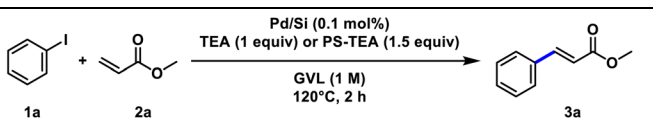


| Entry | Catlyst | Base | $C^b$ (%) | Pd[c] (ppm) |
|---|---|---|---|---|
| 1 | Si_EoLPV | TEA | — | — |
| 2 | Pd/Si | TEA | >99 | 2.6 |
| 3 | Pd/Si | PS-TEA | >99 | 1.9 |
| 4 | Pd/Si[d] | PS-TEA | >99 | 2.9 |
| 5 | Pd/Si_EoLPV | TEA | >99 | 2.7 |
| 6 | Pd/Si_EoLPV | PS-TEA | >99 | 1.6 |
| 7 | Pd/C | TEA | >99 | 8.9 |
| 8 | Pd/C | PS-TEA | >99 | 2.6 |
| 9 | $Pd/SiO_2$[e] | TEA | >99 | 48.0 |
| 10 | $Pd/SiO_2$[e] | PS-TEA | >99 | 9.0 |

[a] Reaction condition: catalysts (0.1 mol%), **1a** (1 mmol), **2a** (1.2 equiv., 1.2 mmol), TEA (1 equiv., 1 mmol) or PS-TEA (1.5 equiv., 1.5 mmol), GVL (0.8 M), 130 °C, 2 h. [b] Conversion was determined by gas–liquid chromatography. The remaining material is unreacted **1a**. [c] Pd leaching determined by MP-AES analysis. [d] GVL (1 M), 120 °C. [e] 16 h. Pd/Si loading 2.7 wt%, Pd/Si_EoLPV loading 3.0 wt%, Pd/C loading 10 wt%, $Pd/SiO_2$ loading 8.7 wt%.

silanol groups (Si–OH). In contrast, the lower surface acidity of the catalyst derived from silicon promotes stronger metal–support interactions and enhances catalytic stability in the presence of organic bases.

Pd leaching in conventional solvents (DMF and DMA) with TEA as base was 11 ppm and 28 ppm, respectively, confirming the better performance in this respect when the catalyst is used in GVL.

The recyclability of Pd/Si and Pd/Si_EoLPV was tested for representative six consecutive runs using both TEA and PS-TEA, yielding a stable complete conversion with a reduced amount of Pd leaching (Fig. 3). To stress the catalyst, the recycle was performed at half conversion with both bases, observing stable conversion over representative five runs (see SI).

Since the removal of Si-based catalysts from PS-TEA after the reaction was not possible, catalyst and base were together both recovered and the Pd/Si/PS-TEA system reused (see the SI for further details). After the reaction, the Pd-catalyst/PS-TEA system was filtered off, and the pure product **3a** was obtained in 92% isolated yield.

After six consecutive runs, the Pd/Si sample was characterised using STEM and EDS, which confirmed the preservation of the Pd nanoparticles; the average particle size was 12.1 ± 4.3 nm (Fig. 4i). XPS analysis exhibits mainly Pd with oxidation states (0) at a binding energy of 336.1 eV and ($2^+$) at 337.7 eV, with a $0/2^+$ ratio of 4.5. The peaks corresponding to the Pd $3d_{5/2}$ and Pd $3d_{3/2}$ orbitals show a DSOC (doublet spin–orbit coupling) of 5.2 eV for both $Pd^0$ and $Pd^{2+}$ (Fig. 4ii).

The catalytic mechanism was investigated *via* hot filtration, mercury poisoning, and half-conversion leaching tests. Leaching values remained constant from half to full conversion, suggesting a robust "release and catch" equilibrium.[59]

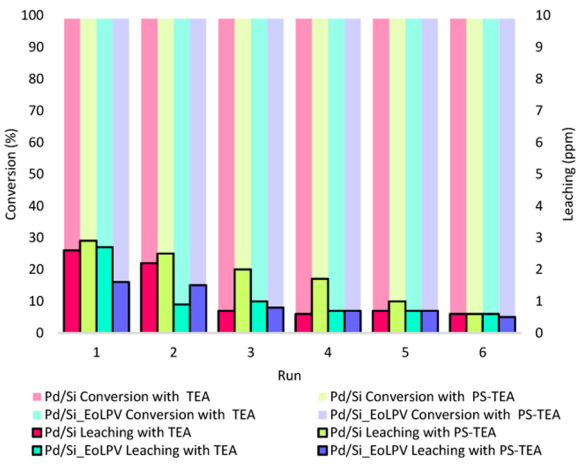


**Fig. 3** Recycle of Pd/Si and Pd/Si_EoLPV using TEA and PS-TEA as bases *versus* Pd leaching (ppm). Reaction condition: catalyst (0.1 mol%), **1a** (1 mmol), **2a** (1.2 equiv., 1.2 mmol), TEA (1 equiv., 1 mmol) or PS-TEA (1.5 equiv., 1.5 mmol), GVL (1 M), 120 °C, 2 h. Conversion was determined by gas–liquid chromatography. The remaining material is unreacted **1a**. Pd leaching determined by MP-AES analysis.

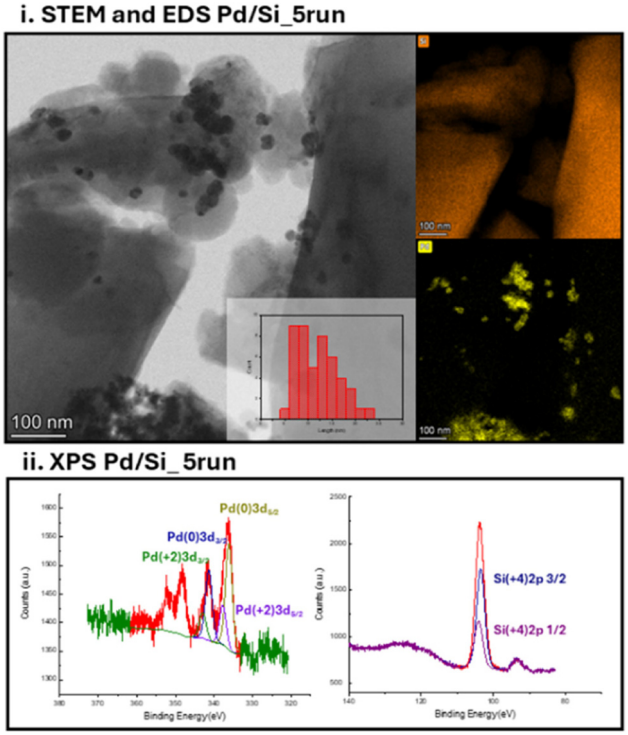


**Fig. 4** (i) STEM and EDS images and nanoparticle size distribution of Pd/Si. (ii) XPS XPS spectrum of Pd 3d region and the Si 2p region for the Pd/Si after 5 consecutive runs.

Taken together with the particle-size growth, mercury poisoning test, and the hot filtration results, these data demonstrate that the process is driven by leached, highly active Pd species that redeposit onto the silicon support (see SI for further details).

The Pd/Si efficiency under the reaction conditions was evaluated using variously functionalized aryl iodides and different olefinic coupling partners. The study demonstrated good tolerance to both electron-donating and electron-withdrawing substituents on the aromatic ring, as well as to various acrylates obtained by extraction with water (**3a–3n**). Among the products, the intermediate for the synthesis of an Lp-$PLA_2$ inhibitor (**3m**) was successfully obtained,[60] along with methyl (*E*)-ferulate (**3n**) (Scheme 1).

Styrene (**4**) was employed in the coupling with various functionalized aryl iodides, obtaining good to excellent yields by precipitation (**5a–5d**) (Scheme 2).

Acrylonitrile (**6a**) and acrylamide (**6b**) were then employed, affording the corresponding products in good yields. Acrylic acid (**6c**) was also used to synthesize cinnamic acid (**7c**). Furthermore, acrylonitrile (**6a**) was applied in the preparation of intermediate **7d**, a key precursor in the synthesis of rilpivirine (Scheme 3).[61]

To demonstrate the catalytic system efficiency on a preparative scale, we carried out the synthesis of product **3a** at a gram scale (10 mmol), achieving an excellent isolated yield of 97%. The *E*-factor value was calculated for the reaction performed at

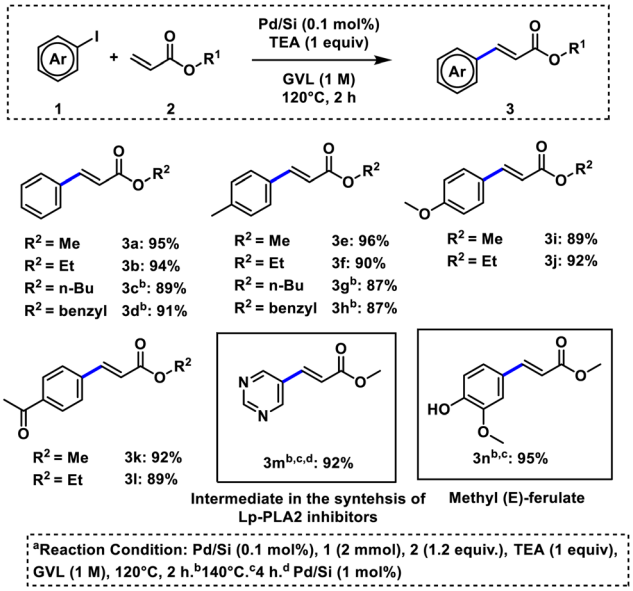


**Scheme 1** Substrate scope with acrylates.

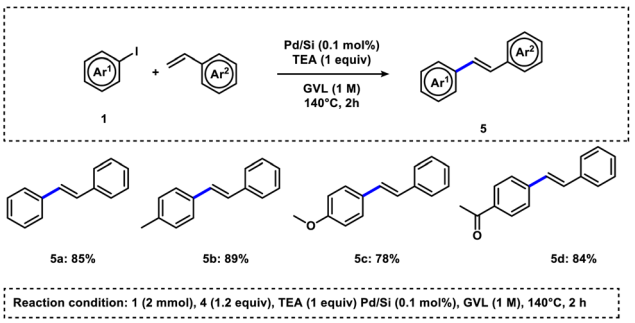


**Scheme 2** Substrate scope with styrene.

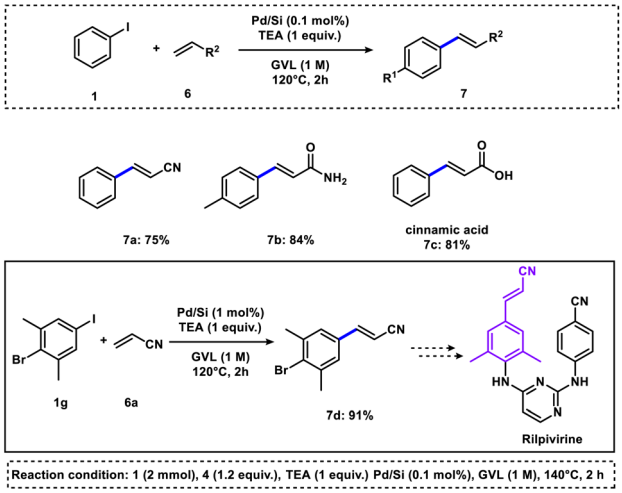


**Scheme 3** Substrate scope with different olefins.

**Table 3** Comparison of TON and TOF

| Entry | Ref. | Catalyst | Run | TON | TOF |
|---|---|---|---|---|---|
| 1 | 47 | Pd/C | 5 | 4100 | 820 |
| 2 | 41 | $Pd/SiO_2$ | 3 | 1807 | 100 |
| 3 | 40 | $Pd_3P$@1P–$SiO_2$ | 3 | 337 | 112 |
| 4 | 62 | $SiO_2$–POSS-imidazolium support | 7 | 8568 | 476 |
| 5 | 42 | Pd–SH–$SiO_2$ | 6 | 552 | 0.6 |
| 6 | This work | Pd/Si | 6 | 5820 | 582 |

the gram scale, obtaining a value of 8.5. The contamination of Pd into the final product was 0.32 ppm, without further purification. The catalyst was subsequently recycled five times at this scale, maintaining complete conversion in every run. In total, we isolated 48.5 mmol of product.

The turnover number (TON) of 5820 and a turnover frequency (TOF) of 582 $h^{-1}$ were obtained for the recycle over six consecutive runs. Comparing our Pd/Si with Pd/C, we observe that the recyclability and TON are comparable and even higher. At the same time, the TOF is half, as we considered a 2 h reaction time to reach fullness at 120 °C instead of 1 h at 150 °C, as reported for Pd/C.[47] The $Pd/SiO_2$ catalyst exhibits reduced recyclability as well as lower TON and TOF, confirming that using silicon significantly improves performance compared to amorphous $SiO_2$.[41] Our Pd/Si system achieves good recyclability, demonstrating the stability of our silicon-based system.[40,42] While the $SiO_2$-POSS-imidazolium support delivers a very high TON,[62] our Pd/Si catalyst provides a superior TON/TOF ratio (Table 3).

## Conclusions

In summary, we have demonstrated an effective upcycling strategy for silicon recovered from End-of-Life photovoltaic panels, utilising it as a support for the preparation of a heterogeneous Pd-based catalyst that is competitive with the widely used commercial Pd/C catalyst. The silicon, obtained by delamination, purified by leaching to remove residual Al and Ag, and subsequently milled, was successfully used to synthesize a novel catalyst, Pd/Si_EoLPV. Its catalytic activity was evaluated in the Mizoroki–Heck coupling using GVL as a preferred green solvent. The recovered Si-based catalyst, Pd/Si_EoLPV, exhibited performance comparable to that of an analogous catalyst prepared from commercial Si powder (Pd/Si) in terms of catalytic efficiency, recyclability, and Pd leaching. The Si-based catalysts remained stable over six consecutive runs, with Pd leaching below 3 ppm. These results correspond to a turnover number (TON) of 5820 and a turnover frequency (TOF) of 582 $h^{-1}$. On a gram scale, the catalyst was applied for 5 recycling cycles, yielding a total of 48.5 mmol of product with an excellent isolated yield of 97% and an *E*-factor of 9. Furthermore, the novel Pd/Si catalyst was successfully applied to the synthesis of 22 substrates from various iodoarenes and olefins, including intermediates relevant to the preparation of rilpivirine, Lp-$PLA_2$ inhibitors, and methyl-2-ferulates. Overall, this work demonstrates the feasibility of upcycling solar-grade

silicon, which is typically not reusable for photovoltaic applications, into an efficient, stable, and recyclable heterogeneous catalyst. This approach not only provides a sustainable alternative to commercial Pd/C but also offers a valuable strategy to extend the lifecycle of a critical and costly material that would otherwise become waste in the coming years.

## Experimental part

### Delamination and recovery of silicon cells

Following the thermomechanical removal of the front glass by heating a panel portion on a hotplate to soften the EVA encapsulant, the photovoltaic panel features a layered EVA/silicon PV cells/EVA/back sheet structure. This portion was then further fragmented into ~1 $cm^2$ pieces, which were added to a reaction flask containing 150 mL of tetrahydrofuran (THF), subjected to reflux, and vigorously stirred at 60 °C for 1 hour. This process induces significant swelling of the EVA layers, causing the crystalline silicon cells to detach and fragment, which then settle to the bottom of the flask. After cooling to room temperature, the swollen EVA and back sheet residues, which float on the solvent surface, were removed *via* coarse filtration. The silicon cells were subsequently recovered by Buchner filtration and washed multiple times with deionised water. Finally, the silicon cells were dried overnight at 60 °C.

### Al and Ag leaching treatment

A conventional two-step leaching process was employed to purify silicon PV cells. Initially, 25 g of Si cells were immersed in 150 mL of 2 M NaOH aqueous solution for 60 minutes, under vigorous stirring. This treatment aimed to dissolve the aluminium back-contact, converting it into soluble sodium aluminate salt. Following this, the solid sample was separated from the leaching solution *via* Buchner filtration and washed several times with deionised water. Subsequently, the second step addressed the dissolution of silver. This was achieved by treating the Si cells in 150 mL of 3 M $HNO_3$ aqueous solution for 60 minutes, under stirring. The silver dissolution resulted in the conversion of silver to soluble silver nitrate. As before, the silicon cells were then separated from the leaching solution *via* Buchner filtration and washed repeatedly with deionised water. Finally, the silicon cells were thermally treated in a muffle furnace at 500 °C for 1 h, yielding 20.281 g of Si powder.

### Preparation of silicon powder by ball milling

A RETSCH High Energy Ball Mill EMAX was employed for the high-energy milling of the purified Si PV cells. For this process, 10 g of silicon cells were placed into a 50 mL tungsten carbide grinding jar containing 100 grinding balls (3 mm diameter). Milling was performed at 800 rpm for 80 minutes.

### Preparation of the catalyst Pd/Si

In a 50 mL two-neck round-bottom flask, 400 mg of the Si support was suspended in 20 mL of diethylene glycol. An aqueous solution of $H_2PdCl_4$ (prepared by dissolving 87 mg of $PdCl_2$ in 1 mL of HCl) was added dropwise under sonication. The pH was adjusted to 12–13 by adding 5 M NaOH solution. The reduction step was carried out at 130 °C for 3 hours under an Ar atmosphere. The suspension was filtered and washed several times with hot water, ethanol, and acetone. The loading of Pd (9.9 wt%) was measured by MP-AES analysis.

### Typical procedure for the Heck–Mizoroki reaction with TEA

In a 4 mL screw-capped vial equipped with a magnetic stirrer, aryl iodide 1 (2.0 mmol), alkene 2–6 (2.4 mmol), GVL (0.8 M, 2.50 mL), triethylamine (2 mmol), and Pd/Si (0.1 mol%, 9.9 wt%) were consecutively added. The resulting mixture was left under stirring at 130 °C. After 2 h, the heterogeneous catalyst was filtered off and washed with 1 mL of GVL. The solvent was distilled and recovered (95%) as a pure solvent, and the product was extracted with 3 mL of heptane. The organic phase was washed with water (3 × 2 mL), and the solvent was removed under vacuum to afford the pure product 3–7.

## Author contributions

The manuscript was written with contributions from all authors. All authors have approved the final version of the manuscript. G. B., M. M., and F. C.: investigation, methodology, data analysis, manuscript preparation–review; N. T. and M. L. P.: silicon recovery methodology, manuscript preparation–review; L. V.: conceptualisation, project administration, manuscript review/editing.

## Conflicts of interest

There are no conflicts to declare.

## Data availability

The data supporting this article have been included as part of the supplementary information (SI). Supplementary information is available. See DOI: https://doi.org/10.1039/d6gc00369a.

## Acknowledgements

This work has been funded by the European Union – NextGenerationEU under the Italian Ministry of University and Research (MUR) National Innovation Ecosystem grant ECS00000041 – VITALITY. We acknowledge Università degli Studi di Perugia and MUR for support within the project Vitality. We acknowledge Università degli Studi di Perugia and MUR for support within the project Vitality. MUR is also thanked for PRIN-2022 project "20223ARWAY – REWIND". The authors gratefully acknowledge Dr Elena Salernitano (ENEA SSPT-TIMAS-MCC) for her support in performing the SEM–

EDX analyses on the silicon powder recovered from end-of-life photovoltaic panels.

## References

1 N. Armaroli and V. Balzani, *Chem. – Eur. J.*, 2016, **22**, 32–57.
2 F. J. M. M. Nijsse, J.-F. Mercure, N. Ameli, F. Larosa, S. Kothari, J. Rickman, P. Vercoulen and H. Pollitt, *Nat. Commun.*, 2023, **14**, 6542.
3 C. Breyer, D. Bogdanov, A. Gulagi, A. Aghahosseini, L. S. N. S. Barbosa, O. Koskinen, M. Barasa, U. Caldera, S. Afanasyeva, M. Child, J. Farfan and P. Vainikka, *Prog. Photovoltaics: Res. Appl.*, 2017, **25**, 727–745.
4 Solar Power Europe, *Global Market Outlook for Solar Power 2025–2029*, 2024.
5 International Renewable Energy Agency, *Renewable Capacity Statistics*, 2023.
6 Md. S. Chowdhury, K. S. Rahman, T. Chowdhury, N. Nuthammachot, K. Techato, Md. Akhtaruzzaman, S. K. Tiong, K. Sopian and N. Amin, *Energy Strategy Rev.*, 2020, **27**, 100431.
7 International Renewable Energy Agency, *End-of-Life Solar PV Panels*, 2016.
8 G. Song, Y. Lu, B. Liu, H. Duan, H. Feng and G. Liu, *J. Environ. Manage.*, 2023, **338**, 117675.
9 B. Al Zaabi and A. Ghosh, *Sol. Energy*, 2024, **283**, 112985.
10 Y. Wei, W. Zhang and J. Gao, *Green Chem.*, 2024, **26**, 5684–5707.
11 K. Li, Y. Qin, D. Zhu and S. Zhang, *Circular Economy*, 2023, **2**, 100025.
12 P. Bhattacharjee, I. Howlader, Md. A. Rahman, H. Md. M. Taqi, Md. T. Hasan, S. M. Ali and M. Alghababsheh, *J. Cleaner Prod.*, 2023, **401**, 136767.
13 V. Kouloumpis, G. E. Konstantzos, C. Chroni, K. Abeliotis and K. Lasaridi, *Sustainable Prod. Consumption*, 2023, **41**, 291–304.
14 European Parliament and of the Council, *Directive 2012/19/EU on WEEE*, 2012.
15 G. A. Heath, T. J. Silverman, M. Kempe, M. Deceglie, D. Ravikumar, T. Remo, H. Cui, P. Sinha, C. Libby, S. Shaw, K. Komoto, K. Wambach, E. Butler, T. Barnes and A. Wade, *Nat. Energy*, 2020, **5**, 502–510.
16 M. Tao, V. Fthenakis, B. Ebin, B. Steenari, E. Butler, P. Sinha, R. Corkish, K. Wambach and E. S. Simon, *Prog. Photovoltaics: Res. Appl.*, 2020, **28**, 1077–1088.
17 I. M. Peters and C. J. Brabec, *Nat. Rev. Chem.*, 2025, **9**, 427–429.
18 R. Deng, N. L. Chang, Z. Ouyang and C. M. Chong, *Renewable Sustainable Energy Rev.*, 2019, **109**, 532–550.
19 J. P. Helveston, G. He and M. R. Davidson, *Nature*, 2022, **612**, 83–87.
20 M. S. W. Lim, D. He, J. S. M. Tiong, S. Hanson, T. C.-K. Yang, T. J. Tiong, G.-T. Pan and S. Chong, *J. Cleaner Prod.*, 2022, **340**, 130796.
21 C. E. L. Latunussa, F. Ardente, G. A. Blengini and L. Mancini, *Sol. Energy Mater. Sol. Cells*, 2016, **156**, 101–111.
22 B. Huang, J. Zhao, J. Chai, B. Xue, F. Zhao and X. Wang, *Sol. Energy*, 2017, **143**, 132–141.
23 M. Calì, B. Hajji, G. Nitto and A. Acri, *Appl. Sci.*, 2022, **12**, 9092.
24 C. Ramírez-Márquez, *Commodities*, 2025, **4**, 18.
25 S. Pizzini, *Sol. Energy Mater. Sol. Cells*, 2010, **94**, 1528–1533.
26 P. R. Dias, L. Schmidt, N. L. Chang, M. Monteiro Lunardi, R. Deng, B. Trigger, L. Bonan Gomes, R. Egan and H. Veit, *Renewable Sustainable Energy Rev.*, 2022, **169**, 112900.
27 O. Wang, Z. Chen and X. Ma, *Green Chem.*, 2024, **26**, 3688–3697.
28 G. Wei, Y. Zhou, Z. Hou, Y. Li, Q. Liu, J. Chen and D. He, *EES Sol.*, 2025, **1**, 9–29.
29 P. Cerchier, F. Miserocchi, L. Pezzato, L. Federzoni, M. L. Protopapa, N. Taurisano, V. Valenzano, M. Amadio, E. Tolusso, F. Marzullo, S. Rosado, S. Onate, L. G. Corral, L. Presa, J. P. Mai, J. Pudack, L. Kruger, S. Rizzato, G. Maruccio and K. Brunelli, *Environ. Eng. Manage. J.*, 2024, **23**, 2041–2050.
30 M. L. Protopapa, E. Burresi, M. Palmisano, E. Pesce, M. Schioppa, L. Capodieci, M. Penza, D. Della Sala, N. Vincenti, A. Accili and L. Campadello, *Resour., Conserv. Recycl.*, 2021, **171**, 105634.
31 R. Yang, N. Zhu, Y. Xi, S. Gao, P. Wu and Z. Dang, *Green Chem.*, 2024, **26**, 7246–7257.
32 M. L. Protopapa, G. Ansanelli, M. Pietrantonio and T. Marco, *Detritus*, 2024, 121–128.
33 Y. Sim, Ankit, Y. B. Tay, D. Ravikumar and N. Mathews, *Nat. Rev. Electr. Eng.*, 2025, **2**, 96–109.
34 E. Markert, I. Celik and D. Apul, *Energies*, 2020, **13**, 3650.
35 J. Deng, D. Luo, K. Rong, Z. Gao, J. Chen, K. Zhao and Z. Yu, *Green Chem.*, 2025, **27**, 7191–7207.
36 F. Campana, F. Valentini, A. Marrocchi and L. Vaccaro, *Biofuel Res. J.*, 2023, **10**, 1989–1998.
37 F. Valentini, B. Di Erasmo, M. Ciani, S. Chen, Y. Gu and L. Vaccaro, *Green Chem.*, 2024, **26**, 4871–4879.
38 F. Valentini, S. Chen, G. Brufani, Y. Gu and L. Vaccaro, *ChemSusChem*, 2024, **18**, e202402011.
39 F. Valentini, F. Ferlin, S. Lilli, A. Marrocchi, L. Ping, Y. Gu and L. Vaccaro, *Green Chem.*, 2021, **23**, 5887–5895.
40 A. Neyyathala, F. Flecken, F. Rang, C. Papke and S. Hanf, *Chem. – Eur. J.*, 2024, **30**, e202302825.
41 L. Huang, Z. Wang, T. P. Ang, J. Tan and P. K. Wong, *Catal. Lett.*, 2006, **112**, 219–225.
42 K. I. Shimizu, S. Koizumi, T. Hatamachi, H. Yoshida, S. Komai, T. Kodama and Y. Kitayama, *J. Catal.*, 2004, **228**, 141–151.
43 F. Ferlin, D. Sciosci, F. Valentini, J. Menzio, G. Cravotto, K. Martina and L. Vaccaro, *Green Chem.*, 2021, **23**, 7210–7218.
44 Y. M. A. Yamada, Y. Yuyama, T. Sato, S. Fujikawa and Y. Uozumi, *Angew. Chem.*, 2014, **126**, 131–135.

 

45 Z. Dong, J. Li, P. Ge and Y. Yang, *Green Chem.*, 2025, **27**, 11914–11927.
46 F. Valentini, G. Brufani, B. Di Erasmo and L. Vaccaro, *Curr. Opin. Green Sustainable Chem.*, 2022, **36**, 100634.
47 G. Strappaveccia, E. Ismalaj, C. Petrucci, D. Lanari, A. Marrocchi, M. Drees, A. Facchetti and L. Vaccaro, *Green Chem.*, 2015, **17**, 365–372.
48 C. Spadetto, C. Hachemi and M. S. Prévot, *Green Chem.*, 2025, **27**, 13529–13557.
49 J. S. Reinhold, J. Pang, B. Zhang, F. E. Kühn and T. Zhang, *Green Chem.*, 2024, **26**, 10661–10686.
50 K. Watanabe, N. Yamagiwa and Y. Torisawa, *Org. Process Res. Dev.*, 2007, **11**, 251–258.
51 K. Watanabe, *Molecules*, 2013, **18**, 3183–3194.
52 U. Azzena, M. Carraro, L. Pisano, S. Monticelli, R. Bartolotta and V. Pace, *ChemSusChem*, 2019, **12**, 40–70.
53 G. de Gonzalo, A. R. Alcántara and P. Domínguez de María, *ChemSusChem*, 2019, **12**, 2083–2097.
54 V. Pace, P. Hoyos, L. Castoldi, P. Domínguez de María and A. R. Alcántara, *ChemSusChem*, 2012, **5**, 1369–1379.
55 C. S. Slater, M. J. Savelski, D. Hitchcock and E. J. Cavanagh, *J. Environ. Sci. Health, Part A: Toxic/Hazard. Subst. Environ. Eng.*, 2016, **51**, 487–494.
56 A. Racha, C. Samanta, S. Sreekantan and B. Marimuthu, *Energy Fuels*, 2023, **37**, 11475–11496.
57 G. Li, N. Li, M. Zheng, S. Li, A. Wang, Y. Cong, X. Wang and T. Zhang, *Green Chem.*, 2016, **18**, 3607–3613.
58 J. L. Osorio-Tejada, F. Ferlin, L. Vaccaro and V. Hessel, *Green Chem.*, 2023, **25**, 9760–9778.
59 C. Calabrese, V. Campisciano, F. Siragusa, L. F. Liotta, C. Aprile, M. Gruttadauria and F. Giacalone, *Adv. Synth. Catal.*, 2019, **361**, 3758–3767.
60 Y. Jin, Z. Wan and Q. Zhang, *US Patent Application* US2012/0142717A1, 2012.
61 D. Schils, F. Stappers, G. Solberghe, R. van Heck, M. Coppens, D. Van den Heuvel, P. Van der Donck, T. Callewaert, F. Meeussen, E. De Bie, K. Eersels and E. Schouteden, *Org. Process Res. Dev.*, 2008, **12**, 530–536.
62 L. Huang, Z. Wang, T. P. Ang, J. Tan and P. K. Wong, *Catal. Lett.*, 2006, **112**, 219–225.